Food and Chemical Toxicology 211 (2026) 115991

Contents lists available at ScienceDirect

Food and Chemical Toxicology

journal homepage: www.elsevier.com/locate/foodchemtox

Subchronic arsenic exposure induced intestinal microbiota dysbiosis and intestinal inflammation via activating the NF-κB signaling pathway

Siyan Cao [b,c,d,1], Runzhi Cai [c,e,1], Shuhua Xi [b,c,d], Yue Wang [a,b,c,*]

[a] School of Public Health, Shenyang Medical College, No. 146 Huanghe North Street, Shenyang, 110034, China
[b] Key Laboratory of Environmental Stress and Chronic Disease Control & Prevention (China Medical University), Ministry of Education, Shenyang, Liaoning, 110122, China
[c] The Key Laboratory of Liaoning Province on Toxic and Biological Effects of Arsenicy, Shenyang, Liaoning, 110122, China
[d] Department of Environmental Health, School of Public Health, China Medical University, Shenyang, Liaoning, 110122, China
[e] Maternal and Child Health Hospital of Gusu District, Suzhou, Jiangsu, 215000, China

ARTICLE INFO

Handling Editor: Professor Matthew Wright

Keywords:
Arsenic
Intestinal flora
Inflammation
NF-κB

ABSTRACT

Arsenic is a prevalent environmental contaminant found in contaminated drinking water. However, the effects of arsenic exposure on the intestinal tract and the specific mechanisms of action remain unclear. In this study, we utilized subchronic sodium arsenite (NaAsO2)-exposed mice and the NaAsO2-treated human colon mucosal epithelial cell line 460 (NCM460) models to investigate the intestinal damage induced by arsenic. Hematoxylin-eosin (HE) staining revealed that the intestines of mice exposed to arsenic exhibited histological damage, characterized by the destruction of epithelial cells, a reduction in the thickness of the muscularis propria, and an increased infiltration of inflammatory cells within the colonic tissue. Mice exposed to arsenic demonstrated a significant reduction in the expression levels of the Occludin protein, accompanied by elevated concentrations of two biomarkers indicative of intestinal barrier damage: serum diamine oxidase (DAO) and lactate (D-LA). Analysis using 16S rRNA sequencing revealed that arsenic exposure did not significantly affect the α and β diversity of the mouse gut microbiota. However, it resulted in changes in the abundance of Clostridiaceae, Burkholderiaceae, Erysipelotrichaceae, and Helicobacteraceae increased, while Muribaculaceae decreased. Furthermore, exposure to arsenic led to increased protein levels of IL-1β, IL-6, and TNF-α, while simultaneously decreasing the expression of IL-10. Arsenic activated NF-κB signaling pathway, which involved in colonic inflammation. Finally, intervention with Pyrrolidine dithiocarbamate (PDTC) significantly attenuated arsenic-induced intestinal inflammation. In conclusion, arsenic exposure compromises the integrity of the intestinal mucosa and disrupts the homeostasis of the intestinal microbiota. Additionally, arsenic mediates intestinal inflammation through the NF-κB signaling pathway.

1. Background

Arsenic, a toxic metalloid, predominantly exists in nature mainly as inorganic and organic arsenic compounds. Human exposure to arsenic primarily occurs through the consumption of groundwater with elevated arsenic levels (Bustaffa et al., 2014). Globally, hundreds of millions of individuals across more than 20 countries—including Bangladesh, India, China, Chile, Argentina, the United States, and Canada—are exposed to varying concentrations of arsenic (Nurchi et al., 2020). An estimated 200 million individuals worldwide have experienced prolonged exposure to arsenic levels exceeding the World Health Organization's safety threshold of 10 μg/L (Naujokas et al., 2013). Prolonged exposure to arsenic has been linked to numerous health problems, encompassing types of cancer along with non-cancerous conditions like cardiovascular diseases, cerebrovascular diseases, type II diabetes, and respiratory disorders (Chen et al., 1992; Jiang et al., 2023; Navas-Acien et al., 2005, 2006). The gastrointestinal tract absorbs 70-90% of ingested inorganic arsenic (iAs) species, which subsequently disseminates through the bloodstream. Major deposition sites include the liver, kidneys, lungs, and bladder (Palma-Lara et al., 2020). The

* Corresponding authorDepartment of Environmental Health, School of Public Health, China Medical University, Shenbei New District, Puhe Road, No.77, Shenyang, Liaoning Province, 110122, China.
E-mail address: yuewang@cmu.edu.cn (Y. Wang).
[1] These authors contributed equally to this work.

https://doi.org/10.1016/j.fct.2026.115991
Received 14 December 2025; Received in revised form 14 January 2026; Accepted 3 February 2026
Available online 5 February 2026

intestinal tract is often overlooked as a target organ for arsenic toxicity. Recently, it was reported that iAs affected intestinal health and damaged the mucosal barrier of the small intestine (Mukherjee et al., 2024; Zhao et al., 2023).

Intestinal microbiota play a crucial role in metabolism, immunity, signaling, and neural development and function. However, they are susceptible to various disruptors, including unhealthy diets, antibiotics, drugs, alcohol, toxic chemicals, and pathogenic bacteria. Dysbiosis of the intestinal microbiota compromises the stability of the intestinal mucosal barrier and disrupts the immune system, leading to oxidative stress and inflammation (Cristofori et al., 2021). Standard culturing methods are ineffective for the majority of gut flora. In contrast, molecular techniques such as 16S rRNA sequencing of intestinal samples enable precise bacterial detection and systematic categorization (Mas-Lloret et al., 2020). The findings from the 16S microbiota analysis can be categorized into two primary components: alpha diversity and beta diversity. Alpha diversity emphasizes the richness and variety of microbiota within a single sample. In contrast, beta diversity analysis is conducted to evaluate the similarity in microbial community composition among different samples, highlighting any significant differences between sample groups. A study indicated that arsenic led to alterations in gut microbial alpha diversity, however, it did not affect beta diversity in mice (Domene et al., 2023). Another investigation found that exposure to arsenic decreased the relative presence of *Akkermansia*, a beneficial intestinal bacterium that helps protect against inflammation in the gut (Yang et al., 2023). Arsenic could result in elevated levels of *Bacteroidetes* and reduced levels of *Firmicutes* in the mouse colon (Dheer et al., 2015). However, it is still unclear whether arsenic-induced intestinal toxicity and inflammation are related to the disruption of the intestinal microbiota.

The transcription factor NF-κB is involved in inflammation and immune response. The NF-κB family comprises p65, Rel B, c-Rel, NF-κB1 (which consists of p50 and its precursor p105), and NF-κB2 (which contains p52 and its precursor p100) (Gadjeva et al., 2007). Among these subunits, p65 plays a crucial role in the expression of a range of pro-inflammatory mediators in most cells (Mitchell et al., 2016). In this study, we investigated the effects of arsenic exposure on dysbiosis of intestinal flora and inflammatory responses, as well as NF-κB signaling pathway activity in the gut. We found that arsenic exposure activated the NF-κB signaling pathway, leading to intestinal inflammation by a combination of in vivo animal experiments and in vitro studies. Our systematic investigation into the effects and mechanisms of arsenic damage to the intestine offers valuable insights, and we identified an active ingredient with potential for intervention, which may serve as a scientific foundation for treating arsenic-induced intestinal damage.

2. Materials and methods

2.1. Animals and treatments

Female Kunming mice that had recently been weaned were acquired from the Experimental Animal Center at China Medical University, following approval from the Animal Ethics Committee of that institution. The mice underwent acclimatization and were provided with food for one week in a regulated environment, characterized by a temperature setting of 20 ± 2 °C, humidity at 55% ± 10%, and a light/dark cycle lasting 12 h each. They were given unrestricted access to drinking water and housed suitably prior to the commencement of the official experiments. The overall duration of the study was 12 weeks. A total of twenty-four mice were randomly assigned to four distinct groups, each receiving different concentrations of $NaAsO_2$ (MERCK, USA, analytical grade) in their drinking water at levels of 0, 20, 40, and 80 mg/L. Throughout the experimental period, the mice were fed ad libitum. The amount of water consumed by the mice was recorded daily, and their body weight was measured weekly. The mice's fur condition and mental status were also observed regularly. After a 12-week exposure period, fecal samples from the mice were collected to prepare smears and detect bacterial colonies. Samples of intestinal epithelium, serum, and urine were collected from mice for subsequent experiments. Approval for all animal research programs was obtained from the Animal Ethics Committee at China Medical University(IACUC numbers: CMU20231128).

2.2. Cell culture and treatments

The NCM460 cell line, derived from human colon mucosal epithelial cells was obtained from the BeNa Culture Collection (Beijing, China) and maintained in 1640 medium (Procell, Wuhan, China), supplemented with 10% fetal bovine serum and 1% penicillin-streptomycin solution (Biological Industries, USA). To determine the optimal exposure concentration and treatment duration for subsequent experiments, we assessed cell viability using the CCK-8 assay kit (#C0039, Beyotime, China). NCM460 cells were exposed to NaAsO2 at concentrations of 0, 4, 8, and 12 μM for a duration of 48 h. In Experiment 2, participants were categorized into four distinct groups: the Control group, the 12 μM NaAsO2 group, the group receiving 10 μM PDTC (a specific inhibitor of NF-κB), and the PDTC pretreatment group. For the PDTC pretreatment group, 10 μM of PDTC (#A106037, Aladdin, China) was administered to the cells for 24 h prior to exposure to 12 μM NaAsO2 for an additional 24 h.

2.3. Colon length and status measurement

The colon was placed on a flat surface, and its length was measured using a ruler. Subsequently, the intestinal tissues were examined under a light microscope.

2.4. Fecal smear

A small amount of fecal specimen was smeared onto a microscope slide, mixed with a drop of distilled water, and the preparation was analyzed under an optical microscope.

2.5. Serum DAO, D-LA level test

Samples were prepared by diluting serum at specified ratios and analyzed according to the protocols outlined in the DAO Assay Kit and the D-LA Assay Kit, both obtained from Jiancheng Bioengineering Institute, China.

2.6. Gut microbiota testing

Genomic DNA from the microbial community was extracted from fecal particles using the PowerSoil DNA Isolation Kit (Mo Bio Laboratories, USA). The V3 and V4 regions of the 16S rRNA gene were amplified via polymerase chain reaction (PCR) using universal primers. The PCR products were then purified, quantified, and normalized to create a sequencing library. The composition of the gut microbiota was analyzed using the Illumina HiSeq sequencing platform, which facilitated the identification of significantly altered microbial communities.

2.7. H&E staining

The prepared paraffin slices were placed in a baking machine at 60 °C for 1 h. Subsequently, they underwent xylene deparaffinization (15 min in xylene I, followed by 15 min in xylene II) and gradient alcohol dehydration (10 min in 100% alcohol II, 5 min in 95% alcohol, 5 min in 90% alcohol, 5 min in 80% alcohol, and 5 min in 70% alcohol). The sections were washed with PBS three times, with each wash lasting 5 min. Subsequently, the sections were stained with hematoxylin for 5 min, differentiated in hydrochloric acid alcohol (100% alcohol I) for a few seconds, and counterstained in tap water for 2 h. The sections were then placed in eosin (C0105S, Beyotime, China) for 5 min. Following

this, they underwent gradient alcohol dehydration (5 min in 70% alcohol, 5 min in 80% alcohol, 5 min in 90% alcohol, 5 min in 95% alcohol, 10 min in 100% alcohol II, 10 min in 100% alcohol I, and 5 min in xylene II, followed by 5 min in xylene I). Finally, the slices were sealed with neutral resin and stored. Scanning was conducted using a high-resolution panoramic imaging system (CS2, Leica, Germany).

2.8. Immunofluorescence staining

The sections of tissue were subjected to deparaffinization and dehydration prior to the subsequent procedures. For the purpose of revealing the target antigens, an epitope retrieval using microwave-assisted heat in citrate buffer (pH 6.0) was conducted. The inactivation of endogenous peroxidase was achieved by applying a 3% hydrogen peroxide solution. To reduce nonspecific binding, tissue sections were incubated for 30 min with 5% BSA prior to an overnight incubation at 4 °C in a humidity-controlled setting with the primary antibody (phospho–NF–κB), diluted at 1:100). The next day, after equilibrating the slides to room temperature, a corresponding HRP-linked secondary antibody was introduced. Nuclear staining was achieved using DAPI, and coverslips were affixed with an anti-fade fluorescence-preserving mounting medium. Fluorescence microscopy with suitable optical filters was employed for image acquisition and analysis.

2.9. Western blotting

Mouse colon tissues and NCM460 cells were harvested and lysed using RIPA buffer (#SB-BR040, share-bio, China) supplemented with phosphatase and protease inhibitors. The resulting lysates were collected, and protein quantification was performed using a BCA kit (#BCA02, DINGGUO, China). SDS-PAGE ((#WLA013a, Wanleibio, China) gel preparation was carried out based on the molecular weights of the proteins, with 30 μg of each protein sample loaded into the wells. Gel electrophoresis was conducted at 140 V for 1 h. Upon completion, proteins were transferred to a 0.45 μm PVDF (#BCA02, Cytiva, USA) membrane via wet transfer at 100 V for 1 h. The membrane was subsequently blocked with 5% skimmed milk powder for 1 h and 30 min. The bands corresponding to the target proteins were excised and placed into their respective primary antibody tubes for incubation over four nights. The following day, the membrane was washed with PBST and incubated with the relevant fluorescent secondary antibody for 1 h. Finally, the bands were analyzed in grayscale using ImageJ software. The antibodies used included the following: NF-κB (Cell Signaling Technology, 1:500), phospho–NF–κB (Cell Signaling Technology, 1:500), IκBα (Proteintech, 1:500), phospho-IκBα (Proteintech, 1:500), IL-10 (Proteintech, 1:500), TNF-α (Proteintech, 1:500), IL-6 (Proteintech, 1:500), IL-1β (Proteintech, 1:500), Occludin (Proteintech, 1:500), Bcl-2 (Sigma, 1:5000), Bax (Sigma, 1:5000), and β-actin (Sigma, 1:5000) as loading control.

2.10. Annexin V-FITC/PI apoptosis detection

The apoptosis assay was carried out following the provided guidelines (KGA1102-100). Afterward, flow cytometric analysis was performed using a BD FACS Celesta instrument (USA).

2.11. Bioinformatics analysis

The Metascape online platform was utilized for conducting KO and KEGG enrichment analyses in order to identify pathways and functional categories that are significantly enriched in relation to the differentially expressed genes.

2.12. Statistical analysis

The experimental data were analyzed using SPSS version 25.0 statistical software. Quantitative data are presented as mean ± standard deviation ($x \pm SD$). A one-way analysis of variance (ANOVA) was performed to compare statistical differences among groups, with intergroup comparisons conducted using the Student-Newman-Keuls (SNK) test. The chi-square trend test was utilized to analyze the trend of intestinal histology scores in relation to the exposure dose. The Kruskal-Wallis test was employed to assess differences in microbiota among groups, with a significance level set at $P < 0.05$.

3. Results

3.1. Arsenic exposure leads to colon damage in mice in vivo

The precise mechanism underlying colon damage caused by arsenic remains poorly understood. To investigate the effects of arsenic on intestinal health, we developed a comprehensive experimental model using female Kunming mice. The subjects were administered drinking water containing varying concentrations of NaAsO2: 0 mg/L, 20 mg/L, 40 mg/L, and 80 mg/L, over a period of 12 weeks (Fig. 1A). Our findings revealed a significant reduction in body weight in the group exposed to 80 mg/L $NaAsO_2$ compared to the control group. Additionally, exposure to both 40 mg/L and 80 mg/L $NaAsO_2$ resulted in a marked reduction in the overall length of the colon (Fig. 1B and C). Further examination of colon images and fecal smears indicated severe crumpling and hemorrhage in the colon lumen. Moreover, fecal analysis showed the presence of deep intestinal epithelial cells exhibiting a honeycomb pattern in the feces of mice exposed to 80 mg/L $NaAsO_2$ (Fig. 1D and E). Subsequently, we assessed the pathological changes in the colon. H&E staining (Fig. 1F) demonstrated that arsenic exposure led to a decrease in the number of epithelial cells, thinning of the muscular layer, and increased infiltration of inflammatory cells within the colon.

3.2. Arsenic exposure damages the intestinal mucosa and disrupts the homeostasis of the intestinal microbiota in mice

Initially, we assessed the concentrations of serum DAO and D-LA in the plasma of mice, which were correlated with the extent of impairment to the intestinal mucosal barrier. In the group exposed to 40 and 80 mg/L arsenic, the levels of DAO and D-LA were significantly elevated (Fig. 2A and B). The protein Occludin, present in the intestinal mucosa, was found to be associated with the severity of injury to the intestinal mucosal barrier, as its expression level decreased in response to greater degrees of damage. We observed that the expression of Occludin declined with increasing arsenic concentrations in a dose-dependent manner, with the expression level of Occludin in mice exposed to 80 mg/L arsenic being lower than that in the control group (Fig. 2C). Subsequently, we analyzed fecal samples, which revealed that fecal smears from mice exposed to 40 mg/L and 80 mg/L arsenic exhibited an increased number of small rod-shaped bacteria and a more disorganized arrangement (Fig. 2D).

The study of microbial diversity employed 16S rRNA sequencing and demonstrated that arsenic exposure did not significantly impact the alpha and beta diversity of bacterial communities in mice (Fig. 2E and F). In the analysis of the abundance of differential bacterial species, we identified changes in the abundance of five bacterial families: *Clostridiaceae, Burkholderiaceae, Erysipelotrichaceae*, and *Helicobacteraceae* exhibited increases, while *Muribaculaceae* showed a decrease. The highest abundances of *Clostridiaceae, Burkholderiaceae,* and *Erysipelotrichaceae* were recorded in the group exposed to 80 mg/L arsenic, whereas the highest abundance of *Helicobacteraceae* was noted in the 40 mg/L arsenic exposure group. Furthermore, *Muribaculaceae* demonstrated a decrease in abundance in both the 40 and 80 mg/L arsenic exposure groups (Fig. 2G).

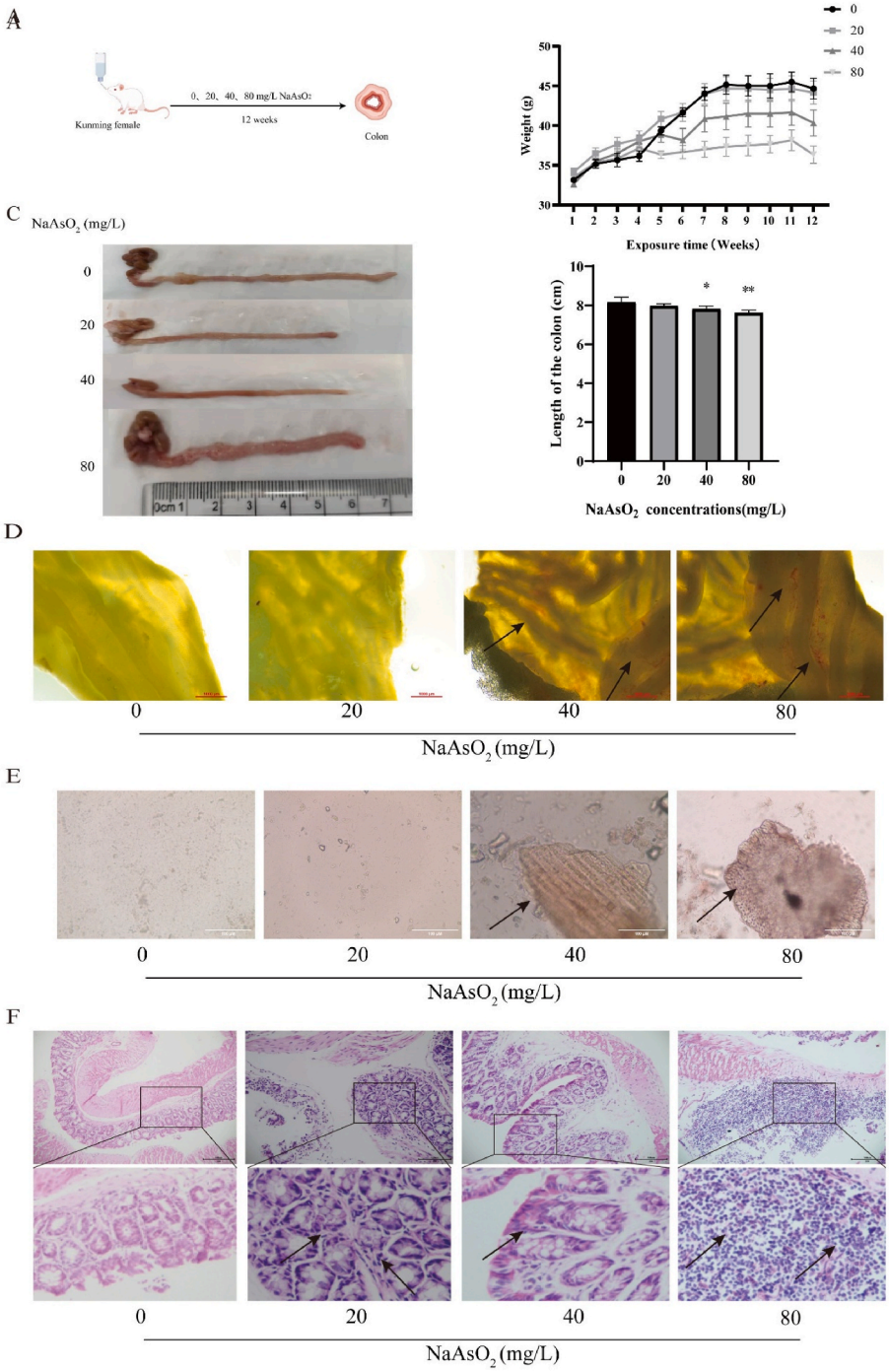

Fig. 1. Arsenic exposure induces colon injury in vivo. **a** Animal model. Kunming mice were exposed to 0, 20, 40, and 80 mg/L $NaAsO_2$ via drinking water for 12 weeks to assess colon injury. **b** Body weight of mice. **c** Colon length in mice (1 cm). **d** Microscopic image of the colon (bar = 1000 μm). **e** Microscopic fecal smear results (bar = 100 μM). **f** H&E staining to observe colon damage (bar = 100 μm). Data are expressed as mean ± SD (n = 4); *$p < 0.05$ and,**$p < 0.01$ compared to the 0 mg/L $NaAsO_2$ group.

3.3. Arsenic exposure induces intestinal inflammatory responses in mice and activates the NF-κB signaling pathway

This research demonstrated that mice exposed to subchronic levels of arsenic exhibited an increase in the protein expression of IL-1β, IL-6, and TNF-α, while the expression of IL-10 was reduced (Fig. 3A). Subsequently, the GSE131032 database was utilized to identify differentially expressed genes in normal mice compared to those with colitis. GO and KEGG enrichment analyses were conducted, showing that the differentially expressed genes were primarily clustered in the inflammatory response function (Fig. 3B). Furthermore, the 25 genes exhibiting the most significant expression differences were selected for heat map analysis. This analysis revealed that the most prominent differentially expressed genes included Dnaaf4, Nfkb1, and Prr29 (Fig. 3C), with the NF-κB1 gene being identified as the most significantly differentially expressed gene in this context. Consequently, we assessed the expression levels of the NF-κB pathway in the intestines of arsenic-exposed mice. The findings indicated that subchronic exposure to arsenic led to an increase in the levels of p–NF–κB and *p*-IκBα, whereas no notable changes were observed in the expression levels of NF-κB and IκBα

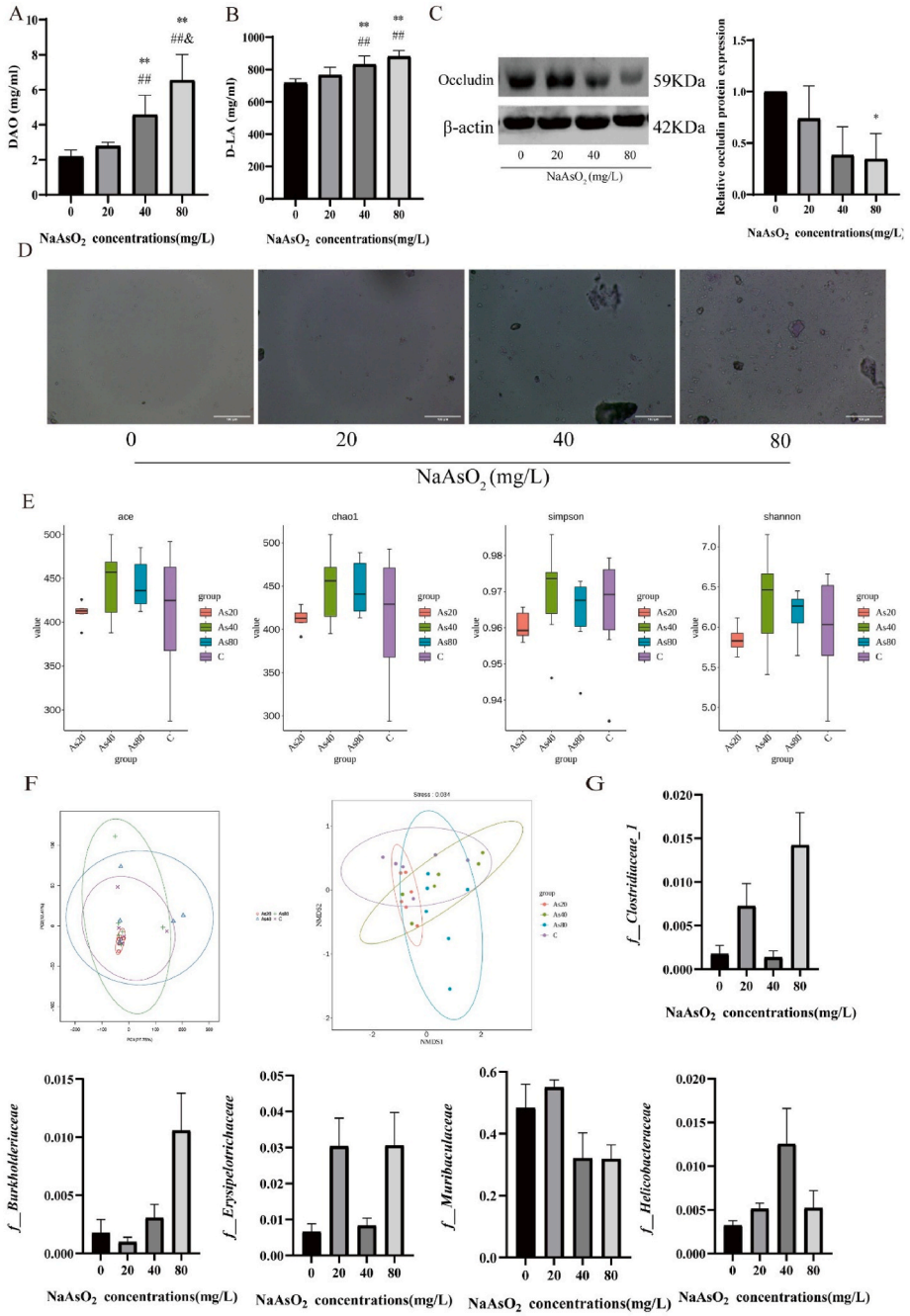

Fig. 2. Arsenic exposure induces colon injury by damaging the intestinal mucosa and disrupting microbiota homeostasis. **a** DAO content. **b** D-LA content. **c** Western blot assay of Occludin levels in mouse colon tissue. **d** Fecal smear analysis (bar = 100 μM). **e** Alpha diversity of the bacterial flora in mice. **f** Beta diversity of the bacterial flora in mice. **g** The abundance of differential bacterial families in mice. Data are expressed as mean ± SD (n = 6); $^{*}p < 0.05$ and $^{**}p < 0.01$ compared to the 0 mg/L $NaAsO_2$ group; $\#p < 0.05$ and $\#\#p < 0.01$ compared to the 20 mg/L $NaAsO_2$ group; & $p < 0.05$ compared to the 40 mg/L $NaAsO_2$ group.

(Fig. 3D and E). Our study demonstrates that arsenic exposure induces intestinal inflammation and activates the NF-κB signaling pathway in mice.

3.4. Arsenic exposure induces intestinal inflammatory responses and activates the NF-κB signaling pathway in vitro

Drawing from the in vivo experimental findings, we established various dose gradients and time-course models to evaluate the impact of arsenic exposure on NCM460 cells. Initially, treatment with 8 and 12 μM $NaAsO_2$ resulted in a significant reduction in cell viability compared to the control cells (Fig. 4A). Consistent with the results observed in arsenic-exposed mice, the expression levels of Occludin in NCM460 cells treated with 8 and 12 μM $NaAsO_2$ were significantly decreased compared to the control cells (Fig. 4B). Furthermore, exposure to $NaAsO_2$ induced an increase in the levels of p–NF–κB and *p*-IκBα, while the expression of IκBα was diminished, with no significant change in NF-κB levels (Fig. 4C). Additionally, the protein levels of IL-1β, IL-6, and TNF-α were markedly elevated in NCM460 cells treated with 8 and 12 μM $NaAsO_2$, accompanied by a notable reduction in IL-10 expression (Fig. 4D). These results corroborate our previous studies conducted on an arsenic-exposed mouse model.

Moreover, we observed apoptosis in NCM460 cells following treatment with arsenic. The concentrations of $NaAsO_2$ at 4, 8, and 12 μM

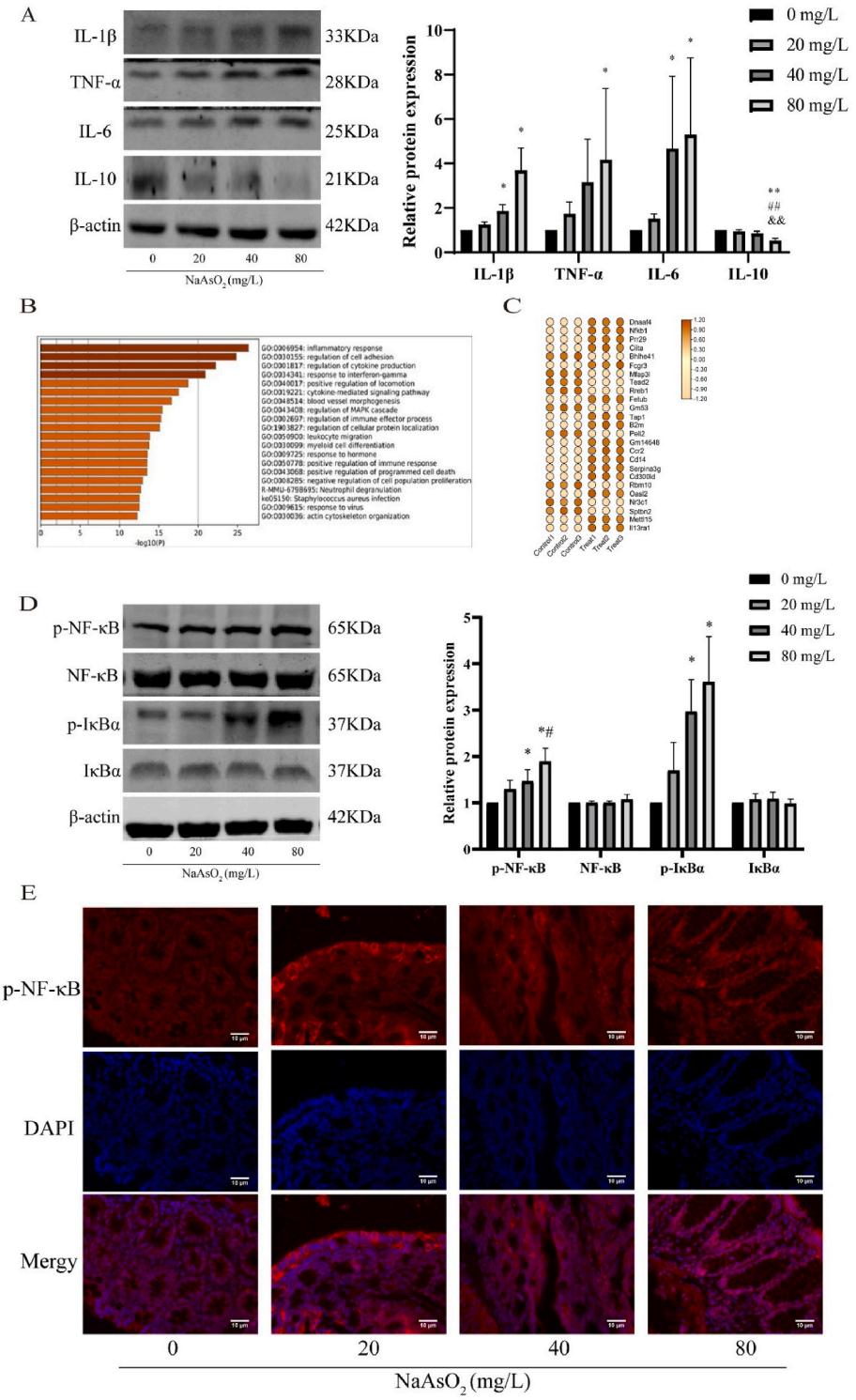

Fig. 3. Arsenic exposure causes intestinal inflammation by affecting the NF-κB signaling pathway. **a** Western blot assay of IL-1β, IL-6, TNF-α and IL-10 levels in mouse colon tissue. **b** GO and KEGG enrichment analysis plot. **c** Heat map of differentially expressed genes. **d** Western blot assay of p–NF–κB, NF-κB, *p*-IκBα, and IκBα levels in mouse colon tissue. **e** Immunofluorescence detection of p–NF–κB levels in mouse colon tissue. Data are expressed as mean ± SD (n = 4); $*p < 0.05$ and $**p < 0.01$ compared to the 0 mg/L $NaAsO_2$ group; $\#p < 0.05$ and $\#\#p < 0.01$ compared to the 20 mg/L $NaAsO_2$ group; & $p < 0.05$ and && $p < 0.01$ compared to the 40 mg/L $NaAsO_2$ group.

significantly reduced the levels of the anti-apoptotic factor Bcl-2 while enhancing the expression of the pro-apoptotic protein Bax (Fig. 4E). The rate of apoptosis in NCM460 cells increased with escalating concentrations of arsenic treatment, as determined by flow cytometry (Fig. 4F).

3.5. NF-κB signaling involved in arsenic-induced inflammation and apoptosis in NCM460 cells

The NF-κB specific inhibitor PDTC was utilized to investigate its role in arsenic-induced intestinal injury. Our findings revealed that pretreatment with 10 μM PDTC significantly alleviated arsenic-induced

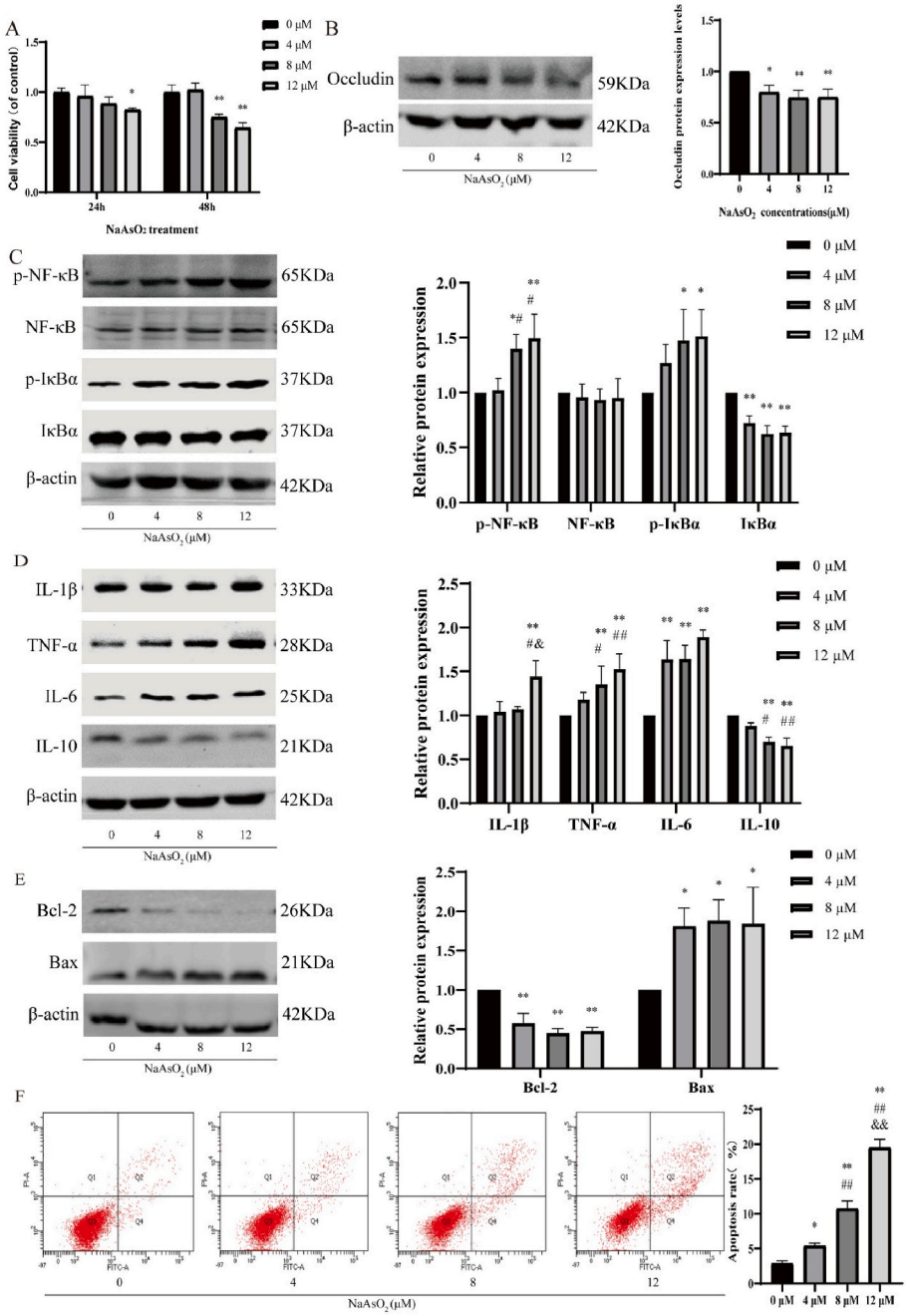

Fig. 4. Arsenic exposure induces enterocyte apoptosis in NCM460 cells in vitro. **a** The CCK-8 assay was used to evaluate the effects of different concentrations of $NaAsO_2$ on the viability of NCM460 cells at 24 h and 48 h **b** The protein levels of occludin in NCM460 cells were measured by Western blot analysis. **c** Western blot assay of p–NF–κB, NF-κB, *p*-IκBα, and IκBα levels in NCM460 cells. **d** Western blot assay of IL-1β, IL-6, TNF-α, and IL-10 in NCM460 cells. **e** Western blot assay of Bcl-2 and Bax in NCM460 cells. **f** Apoptosis levels were assessed by flow cytometry. Data are expressed as mean ± SD (n = 3); $^{*}p < 0.05$ and $^{**}p < 0.01$ compared to the 0 μM $NaAsO_2$ group; $\#p < 0.05$ and $\#\#p < 0.01$ compared to the 4 μM $NaAsO_2$ group; & $p < 0.05$ and && $p < 0.01$ compared to the 8 μM $NaAsO_2$ group.

intestinal damage (Fig. 5A and Fig. S1). In NCM460 cells exposed to 12 μM arsenic, PDTC effectively inhibited the activation of the NF-κB signaling pathway, resulting in a decrease in the arsenic-induced elevation of IL-1β, TNF-α, and IL-6 protein expression, while simultaneously enhancing IL-10 protein expression (Fig. 5B and C). Furthermore, the inhibition of NF-κB by PDTC was associated with increased Bcl-2 levels and a concurrent reduction in Bax expression in arsenic-treated NCM460 cells. Flow cytometry analyses indicated that the administration of PDTC mitigated the rise in apoptosis rate induced by arsenic treatment (Fig. 5D and E). These results suggest that NF-κB signaling is pivotal in the intestinal injury caused by arsenic.

4. Discussion

Recent studies conducted in arsenic-contaminated endemic areas of Latin America indicate that mortality and morbidity related to arsenic exposure continue to rise (Bundschuh et al., 2021). Arsenic poisoning in the human digestive system can cause symptoms such as diarrhea, nausea, vomiting, and irritation (Jomova et al., 2025). Arsenic may harm the intestinal epithelium (Abdul et al., 2015; Ratnaike, 2003). Based on the fact that the most common form of arsenic exposure in the population is chronic arsenite exposure through drinking water, especially the intestinal microbiota of mice has a high degree of similarity with that of humans, we chose to create a mouse model of subchronic

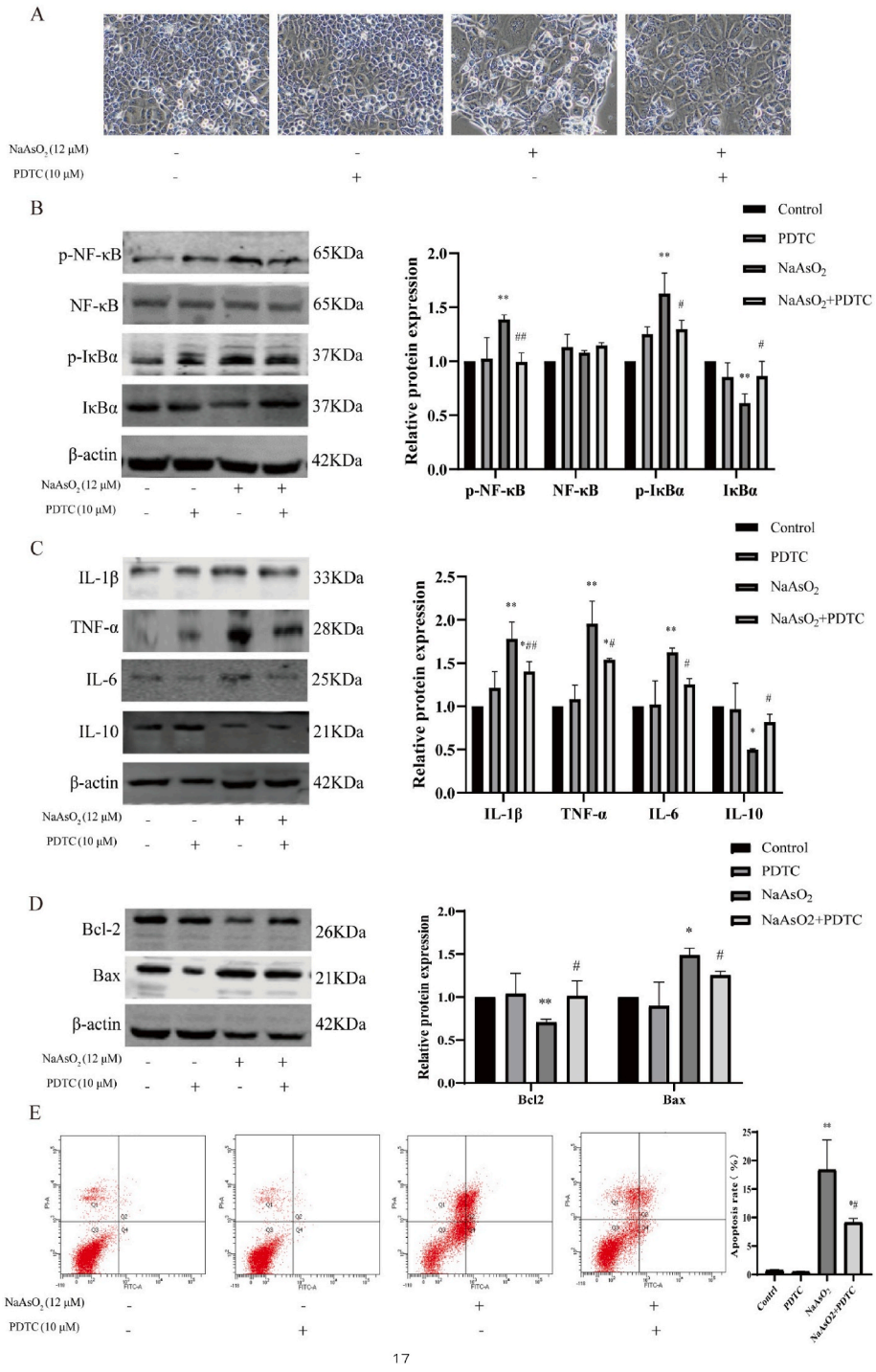

Fig. 5. PDTC attenuates arsenic-induced intestinal inflammatory response by inhibiting the NF-κB signaling pathway. **a** Cell morphology (bar = 20 μM). **b** Western blot assay of p–NF–κB, NF-κB, *p*-IκBα, and IκBα levels in NCM460 cells. **c** Western blot assay of IL-1β, IL-6, TNF-α, and IL-10 in NCM460 cells. **d** Western blot assay of Bcl-2 and Bax in NCM460 cells. **e** Apoptosis levels were assessed by flow cytometry. Data are expressed as mean ± SD (n = 3); $*p < 0.05$ and $**p < 0.01$ compared to the Control group; $\#p < 0.05$ and $\#\#p < 0.01$ compared to the $NaAsO_2$ group.

arsenic exposure by drinking water to study the damage of arsenic on intestinal epithelium and its mechanism. We found that arsenic exposure led to elevated serum levels of DAO and D-LA. Pathological changes in the intestine, as observed through HE staining and corroborated by Western blot results, demonstrate that arsenic can induce intestinal inflammation both in vivo and in vitro.

Epithelial cells are the first line of mucosal defense. In the intestine, a single layer of epithelial cells must establish a selectively permeable barrier that supports nutrient absorption and waste secretion while preventing the leakage of potentially harmful luminal materials. In this study, we observed that arsenic exposure significantly reduced Occludin expression, indicating impaired tight junction function. Although other critical tight junction proteins such as claudins, JAMs, and ZO-1 were not experimentally examined here, their roles in maintaining intestinal barrier integrity are well-established(Kuo et al., 2022; Ugalde-Silva et al., 2016). Future studies should include these markers to provide a more holistic assessment of arsenic-induced barrier dysfunction.

We employed bioinformatics to analyze differential gene expression

associated with inflammatory responses in both control and colitis mice. The gene that exhibited the most significant differential expression in the context of the inflammatory response was NF-κB1. Previous research has demonstrated that arsenic may initiate inflammatory responses in cells by promoting oxidative stress and activating MAPK and NF-κB pathways. The IκB/NFκB signaling network integrates signals from the tumor necrosis factor receptor (TNFR), the toll-like receptor (TLR) superfamily, interleukin receptor (IL-1R), as well as metabolic genotoxicity and shear stress, resulting in transcriptional responses that are specific to signals, environments, and cell types (Mitchell et al., 2016). NF-κB proteins consist of p65 and p50 subunits bound to the inhibitory protein IκB, forming a trimeric complex that remains in an inactivated state in the cytoplasm (Yin and Yu, 2018). After IκB is phosphorylated, the NF-κB dimer disassociates, moves from the cytoplasm into the nucleus, and attaches to specific DNA sequences to enhance the transcription of associated genes (Phookphan et al., 2017). Studies have demonstrated a significant association between gut microbiota and the NF-κB signaling pathway. For example, *Helicobacter pylori* can indirectly activate the NF-κB pathway during the process of gastric carcinogenesis (Van den Abbeele et al., 2018). In contrast, Erysipelotrichaceae upregulates this pathway to enhance intestinal barrier function and activate immune responses(Săsăran et al., 2021). IKBα is located upstream of NK-κB, degrades and prevents activation of NF-κB signaling. The NF-κB signaling pathway plays a pivotal role in regulating the production of pro-inflammatory cytokines, including TNF-α and IL-6, which are essential for the initiation and maintenance of inflammatory responses (Shi et al., 2025). In the regulation of intestinal inflammation, key cytokines often display multifaceted and complex roles. For instance, TNF-α can enhance the survival of intestinal cells by activating the nuclear factor kappa-light-chain-enhancer of NF-κB signaling pathway (Ruder et al., 2019); conversely, it also contributes to inflammatory damage. Experimental evidence demonstrates that in dextran sulfate sodium (DSS)-induced colitis models, the neutralization of IL-6 and TNF-α significantly reduces intestinal permeability and improves barrier function(Xiao et al., 2016). Subsequent intervention using PDTC, an inhibitor of NF-κB, was conducted to evaluate the role of the NF-κB signaling pathway in arsenic-induced intestinal inflammation. The addition of PDTC in vitro resulted in an improvement of arsenic-induced intestinal inflammation. Our findings indicate that arsenic can contribute to intestinal inflammation both in vivo and in vitro by activating the NF-κB signaling pathway.

Gut microbes are susceptible to environmental chemicals, such as arsenic, which can lead to ecological dysregulation of the intestinal epithelium(Tikka et al., 2020). Short-term acute arsenic exposure has been shown to alter the diversity of the microbiome and the distribution of bacterial taxa. However, the effects on the bacterial flora vary depending on the dosage and duration of exposure (Dutta et al., 2018; Zhang et al., 2018). The core pathogen within the family Helicobacteraceae, *Helicobacter pylori*, establishes its pathogenicity through a series of crucial survival mechanisms. It not only adapts to the highly acidic environment of the stomach via specific physiological strategies, but also exhibits targeted motility and adheres firmly to the gastric mucosa(Ansari and Yamaoka, 2019; de Brito et al., 2019). More significantly, its impact lies in the long-term chronic inflammation it mediates. This sustained inflammatory response serves as a key pathological foundation for the development of gastric cancer and gastric mucosa-associated lymphoid tissue (MALT) lymphoma(Zheng et al., 2024). Muribaculaceae is a significant group of beneficial gut commensal bacteria that play a crucial role in maintaining intestinal homeostasis (Zhu et al., 2024). A reduction in their abundance is considered a marker of intestinal dysbiosis and is associated with the onset of various chronic inflammatory and metabolic diseases. Erysipelotrichaceae plays a significant role in maintaining intestinal homeostasis; however, its elevated abundance has been linked to various pathologies. Notably, this family of bacteria is enriched in patients with colorectal cancer and is found to be increased in murine models of inflammatory bowel disease (IBD) (Chen et al., 2012; Schaubeck et al., 2016). In patients with ulcerative colitis and Crohn's disease, the genus Burkholderia exhibits a significant enrichment within the gut microbiota(Masoodi et al., 2019). The family Clostridiaceae plays a dual role in the gut microbiota: its beneficial members are essential for host health, while opportunistic pathogens, such as *Clostridium difficile*, are significant contributors to intestinal infections and inflammation (Brayan et al., 2025). Consequently, fecal flora analysis was conducted in this experiment. The 16S rRNA high-throughput sequencing technique allows for a comprehensive analysis of gut bacteria, revealing their characteristics in various disease states(Momozawa et al., 2011). The results indicated that subchronic arsenic exposure had a minor effect on the alpha and beta diversity of the flora. However, the abundance of five bacterial families—*Helicobacteraceae*, *Muribaculaceae*, *Erysipelotrichaceae*, *Burkholderiaceae*, and *Clostridiaceae*—exhibited significant changes. Subchronic arsenic exposure induces dysbiosis of the gut microbiota, characterized by an increase in pro-inflammatory bacteria and a decrease in beneficial bacteria, thereby establishing a microbial ecological foundation that drives intestinal inflammation. Specifically, this dysbiosis is manifested by the enrichment of pro-inflammatory Helicobacteraceae, a reduction in Muribaculaceae—which is essential for barrier maintenance and anti-inflammatory functions—a dysbiotic shift in Erysipelotrichaceae resembling that observed in metabolic disorders, a marked increase in Burkholderiaceae, which signifies severe ecological imbalance and is directly linked to inflammation, and the disruption of Clostridiaceae homeostasis. Collectively, these alterations synergistically contribute to the initiation and progression of intestinal inflammation through multiple mechanisms.

In this study, we observed that arsenic exposure altered the abundance of several bacterial families, including increases in Clostridiaceae, Burkholderiaceae, Erysipelotrichaceae, and Helicobacteraceae, and a decrease in Muribaculaceae. While our analysis focused on taxonomic shifts, these changes likely correspond to functional alterations in the gut microbiome. For instance, Clostridiaceae and Muribaculaceae are known to be involved in the fermentation of dietary fibers and production of short-chain fatty acids (SCFAs) such as butyrate, which play crucial roles in maintaining intestinal barrier function and exerting anti-inflammatory effects. A reduction in SCFA-producing bacteria could compromise mucosal integrity and promote inflammation, potentially synergizing with arsenic-induced NF-κB activation. Although we did not measure SCFAs or other microbial metabolites in this study, future investigations should incorporate metabolomic profiling to directly link arsenic-induced dysbiosis with functional metabolic disruptions and their contribution to intestinal pathophysiology.

Our experiment is the first to validate the dose-response relationship between arsenic and intestinal inflammation using a female Kunming mouse model. However, this study has certain limitations. First, the selection of female mice as experimental subjects was primarily based on our research group's previous findings, which indicated that arsenic can cause liver and kidney damage in female mice. This prompted further investigation into the effects of arsenic on intestinal health. The gender of the subjects is indeed a crucial factor influencing arsenic susceptibility, and future studies will further explore the effects of arsenic on mice of different genders. Second, the arsenic concentrations in the drinking water provided to the mice were set at 20, 40, and 80 mg/L, significantly exceeding the concentrations typically found in arsenic-contaminated areas (0.2 mg/L). To account for interspecies variation, a safety factor of 100 was applied, resulting in a difference of 20 mg/L in arsenic concentration for the low-concentration group. Furthermore, the duration of arsenic exposure for the mice in this experiment was 12 weeks. Considering that populations residing in arsenic-contaminated areas are exposed to arsenic over prolonged periods, both a medium-dose group (40 mg/L) and a high-dose group (80 mg/L) were established based on the 20 mg/L concentration. Third, the 16S rRNA sequencing method only identifies bacterial species or genera, but not differentiates between live and dead bacteria. Due to the lack of

population-based epidemiological data in this study, extrapolating the results to the general population is challenging. It should be noted that this study is based on animal and cellular models, and lacks direct epidemiological data from human populations exposed to arsenic. However, existing epidemiological studies have reported a higher incidence of gastrointestinal symptoms, mucosal lesions, and inflammatory bowel conditions in individuals from arsenic-endemic regions (Brabec et al., 2020), which is consistent with the pathological changes observed in our experimental models. Future population-based studies are warranted to validate whether the NF-κB–mediated dysbiosis and inflammation pathway identified here also operates in humans chronically exposed to arsenic.

5. Conclusion

In conclusion, arsenic exposure induces dysbiosis of the gut microbiota and intestinal inflammation. The NF-κB signaling pathway plays a crucial role in the intestinal inflammation induced by arsenic exposure. Intervention with PDTC can alleviate arsenic-induced intestinal inflammation. This study not only elucidates the molecular mechanisms underlying arsenic-induced intestinal damage but also identifies an effective intervention component, thereby providing a basis for preventing arsenic poisoning.

CRediT authorship contribution statement

Siyan Cao: Methodology, Investigation, Data curation. **Runzhi Cai:** Methodology. **Shuhua Xi:** Project administration, Funding acquisition, Conceptualization. **Yue Wang:** Writing – review & editing, Project administration, Conceptualization.

Funding

This work was supported by the National Natural Science Foundation of China (No. 81972982).

Declaration of competing interest

The authors declare that they have no known competing financial interests or personal relationships that could have appeared to influence the work reported in this paper.

Appendix A. Supplementary data

Supplementary data to this article can be found online at https://doi.org/10.1016/j.fct.2026.115991.

Data availability

Data will be made available on request.

References

Abdul, K.S., Jayasinghe, S.S., Chandana, E.P., Jayasumana, C., De Silva, P.M., 2015. Arsenic and human health effects: a review. Environ. Toxicol. Pharmacol. 40, 828–846.
Ansari, S., Yamaoka, Y., 2019. Helicobacter pylori virulence factors exploiting gastric colonization and its pathogenicity. Toxins 11.
Brabec, J.L., Wright, J., Ly, T., Wong, H.T., McClimans, C.J., Tokarev, V., Lamendella, R., Sherchand, S., Shrestha, D., Uprety, S., Dangol, B., Tandukar, S., Sherchand, J.B., Sherchan, S.P., 2020. Arsenic disturbs the gut microbiome of individuals in a disadvantaged community in Nepal. Heliyon 6, e03313.
Brayan, M.T., Alejandro, A.A., Quesada-Gómez, C., Chaves-Olarte, E., Elías, B.C., 2025. Polymorphonuclear neutrophil depletion in ileal tissues reduces the immunopathology induced by Clostridioides difficile toxins. Anaerobe 92, 102947.
Bundschuh, J., Schneider, J., Alam, M.A., Niazi, N.K., Herath, I., Parvez, F., Tomaszewska, B., Guilherme, L.R.G., Maity, J.P., López, D.L., Cirelli, A.F., Pérez-Carrera, A., Morales-Simfors, N., Alarcón-Herrera, M.T., Baisch, P., Mohan, D., Mukherjee, A., 2021. Seven potential sources of arsenic pollution in Latin America and their environmental and health impacts. Sci. Total Environ. 780, 146274.
Bustaffa, E., Stoccoro, A., Bianchi, F., Migliore, L., 2014. Genotoxic and epigenetic mechanisms in arsenic carcinogenicity. Arch. Toxicol. 88, 1043–1067.
Chen, C.J., Chen, C.W., Wu, M.M., Kuo, T.L., 1992. Cancer potential in liver, lung, bladder and kidney due to ingested inorganic arsenic in drinking water. Br. J. Cancer 66, 888–892.
Chen, W., Liu, F., Ling, Z., Tong, X., Xiang, C., 2012. Human intestinal lumen and mucosa-associated microbiota in patients with colorectal cancer. PLoS One 7, e39743.
Cristofori, F., Dargenio, V.N., Dargenio, C., Miniello, V.L., Barone, M., Francavilla, R., 2021. Anti-inflammatory and immunomodulatory effects of probiotics in gut inflammation: a door to the body. Front. Immunol. 12, 578386.
de Brito, B.B., da Silva, F.A.F., Soares, A.S., Pereira, V.A., Santos, M.L.C., Sampaio, M.M., Neves, P.H.M., de Melo, F.F., 2019. Pathogenesis and clinical management of Helicobacter pylori gastric infection. World J. Gastroenterol. 25, 5578–5589.
Dheer, R., Patterson, J., Dudash, M., Stachler, E.N., Bibby, K.J., Stolz, D.B., Shiva, S., Wang, Z., Hazen, S.L., Barchowsky, A., Stolz, J.F., 2015. Arsenic induces structural and compositional colonic microbiome change and promotes host nitrogen and amino acid metabolism. Toxicol. Appl. Pharmacol. 289, 397–408.
Domene, A., Orozco, H., Rodríguez-Viso, P., Monedero, V., Zúñiga, M., Vélez, D., Devesa, V., 2023. Intestinal homeostasis disruption in mice chronically exposed to arsenite-contaminated drinking water. Chem. Biol. Interact. 373, 110404.
Dutta, S., Saha, S., Mahalanobish, S., Sadhukhan, P., Sil, P.C., 2018. Melatonin attenuates arsenic induced nephropathy via the regulation of oxidative stress and inflammatory signaling cascades in mice. Food Chem. Toxicol. : an international journal published for the British Industrial Biological Research Association 118, 303–316.
Gadjeva, M., Wang, Y., Horwitz, B.H., 2007. NF-kappaB p50 and p65 subunits control intestinal homeostasis. Eur. J. Immunol. 37, 2509–2517.
Jiang, E.X., Domingo-Relloso, A., Abuawad, A., Haack, K., Tellez-Plaza, M., Fallin, M.D., et al., 2023. Arsenic exposure and epigenetic aging: the association with cardiovascular disease and all-cause mortality in the strong heart study. Environ. Health Perspect. 131, 127016.
Jomova, K., Alomar, S.Y., Nepovimova, E., Kuca, K., Valko, M., 2025. Heavy metals: toxicity and human health effects. Arch. Toxicol. 99, 153–209.
Kuo, W.T., Odenwald, M.A., Turner, J.R., Zuo, L., 2022. Tight junction proteins occludin and ZO-1 as regulators of epithelial proliferation and survival. Ann. N. Y. Acad. Sci. 1514, 21–33.
Mas-Lloret, J., Obón-Santacana, M., Ibáñez-Sanz, G., Guinó, E., Pato, M.L., Rodriguez-Moranta, F., Mata, A., García-Rodríguez, A., Moreno, V., Pimenoff, V.N., 2020. Gut microbiome diversity detected by high-coverage 16S and shotgun sequencing of paired stool and colon sample. Sci. Data 7, 92.
Masoodi, I., Alshanqeeti, A.S., Ahmad, S., Alyamani, E.J., Al-Lehibi, A.A., Qutub, A.N., Alsayari, K.N., Alomair, A.O., 2019. Microbial dysbiosis in inflammatory bowel diseases: results of a metagenomic study in Saudi Arabia. Minerva Gastroenterol. Dietol. 65, 177–186.
Mitchell, S., Vargas, J., Hoffmann, A., 2016. Signaling via the NFκB system. Wiley interdisciplinary reviews. Systems biology and medicine 8, 227–241.
Momozawa, Y., Deffontaine, V., Louis, E., Medrano, J.F., 2011. Characterization of bacteria in biopsies of colon and stools by high throughput sequencing of the V2 region of bacterial 16S rRNA gene in human. PLoS One 6, e16952.
Mukherjee, S., Bhattacharya, R., Sarkar, O., Islam, S., Biswas, S.R., Chattopadhyay, A., 2024. Gut microbiota perturbation and subsequent oxidative stress in gut and kidney tissues of zebrafish after individual and combined exposure to inorganic arsenic and fluoride. Sci. Total Environ. 957, 177519.
Naujokas, M.F., Anderson, B., Ahsan, H., Aposhian, H.V., Graziano, J.H., Thompson, C., Suk, W.A., 2013. The broad scope of health effects from chronic arsenic exposure: update on a worldwide public health problem. Environ. Health Perspect. 121, 295–302.
Navas-Acien, A., Sharrett, A.R., Silbergeld, E.K., Schwartz, B.S., Nachman, K.E., Burke, T. A., et al., 2005. Arsenic exposure and cardiovascular disease: a systematic review of the epidemiologic evidence. Am. J. Epidemiol. 162, 1037–1049.
Navas-Acien, A., Silbergeld, E.K., Streeter, R.A., Clark, J.M., Burke, T.A., Guallar, E., 2006. Arsenic exposure and type 2 diabetes: a systematic review of the experimental and epidemiological evidence. Environ. Health. Perspect. 114, 641–648.
Nurchi, V.M., Djordjevic, A.B., Crisponi, G., Alexander, J., Bjørklund, G., Aaseth, J., 2020. Arsenic toxicity: molecular targets and therapeutic agents. Biomolecules 10.
Palma-Lara, I., Martínez-Castillo, M., Quintana-Pérez, J.C., Arellano-Mendoza, M.G., Tamay-Cach, F., Valenzuela-Limón, O.L., García-Montalvo, E.A., Hernández-Zavala, A., 2020. Arsenic exposure: a public health problem leading to several cancers. Regul. Toxicol. Pharmacol. 110, 104539. RTP.
Phookphan, P., Navasumrit, P., Waraprasit, S., Promvijit, J., Chaisatra, K., Ngaotepprutaram, T., Ruchirawat, M., 2017. Hypomethylation of inflammatory genes (COX2, EGR1, and SOCS3) and increased urinary 8-nitroguanine in arsenic-exposed newborns and children. Toxicol. Appl. Pharmacol. 316, 36–47.
Ratnaike, R.N., 2003. Acute and chronic arsenic toxicity. Postgrad. Med. J. 79, 391–396.
Ruder, B., Atreya, R., Becker, C., 2019. Tumour necrosis factor alpha in intestinal homeostasis and gut related diseases. Int. J. Mol. Sci. 20.
Săsăran, M.O., Meliț, L.E., Dobru, E.D., 2021. MicroRNA modulation of host immune response and inflammation triggered by Helicobacter pylori. Int. J. Mol. Sci. 22.
Schaubeck, M., Clavel, T., Calasan, J., Lagkouvardos, I., Haange, S.B., Jehmlich, N., Basic, M., Dupont, A., Hornef, M., von Bergen, M., Bleich, A., Haller, D., 2016. Dysbiotic gut microbiota causes transmissible Crohn's disease-like ileitis independent of failure in antimicrobial defence. Gut 65, 225–237.
Shi, S., Ou, X., Liu, C., Li, R., Zheng, Q., Hu, L., 2025. NF-κB signaling and the tumor microenvironment in osteosarcoma: implications for immune evasion and therapeutic resistance. Front. Immunol. 16, 1518664.

Tikka, C., Manthari, R.K., Ommati, M.M., Niu, R., Sun, Z., Zhang, J., Wang, J., 2020. Immune disruption occurs through altered gut microbiome and NOD2 in arsenic induced mice: correlation with colon cancer markers. Chemosphere 246, 125791.
Ugalde-Silva, P., Gonzalez-Lugo, O., Navarro-Garcia, F., 2016. Tight junction disruption induced by type 3 secretion System effectors injected by enteropathogenic and enterohemorrhagic Escherichia coli. Front. Cell. Infect. Microbiol. 6, 87.
Van den Abbeele, P., Taminiau, B., Pinheiro, I., Duysburgh, C., Jacobs, H., Pijls, L., Marzorati, M., 2018. Arabinoxylo-Oligosaccharides and Inulin impact inter-individual variation on microbial metabolism and composition, which immunomodulates human cells. J. Agric. Food Chem. 66, 1121–1130.
Xiao, Y.T., Yan, W.H., Cao, Y., Yan, J.K., Cai, W., 2016. Neutralization of IL-6 and TNF-α ameliorates intestinal permeability in DSS-induced colitis. Cytokine 83, 189–192.
Yang, J.L., Juhasz, A.L., Li, M.Y., Ding, J., Xue, X.M., Zhou, D., Ma, L.Q., Li, H.B., 2023. Chronic exposure to drinking water As, Pb, and Cd at provisional guideline values reduces weight gain in Male mice via gut Microflora alterations and intestinal inflammation. Environ. Sci. Technol. 57, 12981–12990.
Yin, L., Yu, X., 2018. Arsenic-induced apoptosis in the p53-proficient and p53-deficient cells through differential modulation of NFkB pathway. Food Chem. Toxicol. : an international journal published for the British Industrial Biological Research Association 118, 849–860.
Zhang, J., Zhang, Y., Wang, W., Li, C., Zhang, Z., 2018. Double-sided personality: effects of arsenic trioxide on inflammation. Inflammation 41, 1128–1134.
Zhao, D., Jiao, S., Yi, H., 2023. Arsenic exposure induces small intestinal toxicity in mice by barrier damage and inflammation response via activating RhoA/ROCK and TLR4/Myd88/NF-κB signaling pathways. Toxicol. Lett. 384, 44–51.
Zheng, H., Zhang, T., Zhang, J., Ning, J., Fu, W., Wang, Y., Shi, Y., Wei, G., Zhang, J., Chen, X., Ding, S., 2024. AUF1-mediated inhibition of autophagic lysosomal degradation contributes to CagA stability and Helicobacter pylori-induced inflammation. Gut Microbes 16, 2382766.
Zhu, Y., Chen, B., Zhang, X., Akbar, M.T., Wu, T., Zhang, Y., Zhi, L., Shen, Q., 2024. Exploration of the Muribaculaceae family in the Gut Microbiota: diversity, metabolism, and function. Nutrients 16.